DOI 10.26724/2079-8334-2025-4-94-189-194
UDC 616.34-006.6:611.438:577.1:546.96/97/98

S.B. Kramar, I.Ya. Andriichuk, S.O. Lytvynyuk, S.Yu. Soroka, Z.M. Nebesna
I. Horbachevsky Ternopil National Medical University, Ternopil

OXIDATIVE STRESS AND THYMUS MORPHOLOGY IN COLON CARCINOGENESIS UNDER THE INFLUENCE OF AU/AG/FE NANOCOMPOSITE

e-mail: kramarsb@tdmu.edu.ua

The purpose of the study was to determine the effect of the Au/Ag/Fe nanocomposite on oxidative stress indicators and the histological state of the thymus under conditions of induced carcinogenesis.

N, N-dimethylhydrazine-induced carcinogenesis triggers pronounced oxidative stress in the thymus, demonstrated by significant increases in lipid and protein peroxidation markers: diene and triene conjugates and thiobarbituric acid reactive substances rose 1.30-, 1.22-, and 2.79-fold, respectively, while Schiff bases increased 2.01-fold. This oxidative damage is accompanied by suppression of the thymic antioxidant system, with reductions in superoxide dismutase, catalase, reduced glutathione, glutathione peroxidase, and glutathione reductase activities, indicating impaired redox homeostasis. Administration of an Au/Ag/Fe nanocomposite during carcinogenesis partially attenuated oxidative stress, led to restored antioxidant enzyme activities, and increasing of thymocyte density by 1.16-fold, suggesting both antioxidant and immunoprotective effects. These findings support further investigation of nanocomposites in mitigating thymic dysfunction under neoplastic conditions.

Key words: oxidative stress, Au/Ag/Fe nanoparticles, thymus, N, N-dimethylhydrazine dihydrochloride, induced colon carcinogenesis.

С.Б. Крамар, І.Я. Андрійчук, С.О. Литвинюк, С.Ю. Сорока, З.М. Небесна

ОКСИДАТИВНИЙ СТРЕС І МОРФОЛОГІЯ ТИМУСА ПРИ КАНЦЕРОГЕНЕЗІ ТОВСТОЇ КИШКИ ТА ДІЇ НАНОКОМПОЗИТУ AU/AG/FE

Метою дослідження було визначити вплив нанокомпозиту Au/Ag/Fe на показники оксидативного стресу та гістологічний стан тимуса в умовах індукованого канцерогенезу. Канцерогенез, індукований N, N-диметилгідразином, викликає виражений оксидативний стрес у тимусі, що проявляється значним збільшенням маркерів перекисного окислення ліпідів та білків: кількість дієнових та трієнових кон'югатів та речовин, що реагують з тіобарбітуровою кислотою, зросла в 1,30, 1,22 та 2,79 раза відповідно, тоді як кількість основ Шиффа збільшилася в 2,01 раза. Це оксидативне пошкодження супроводжується пригніченням антиоксидантної системи тимуса зі зниженням активності супероксиддисмутази, каталази, відновленого глутатіону, глутатіонпероксидази та глутатіонредуктази, що вказує на порушення окисно-відновного гомеостазу. Введення нанокомпозиту Au/Ag/Fe тваринам з індукованим канцерогенезом частково послабило оксидативний стрес, призвело до відновлення активності антиоксидантних ферментів та збільшення щільності тимоцитів у 1,16 раза, що свідчить як про антиоксидантний, так і про імунопротекторний ефект. Ці результати підтверджують необхідність подальшого дослідження нанокомпозитів для пом'якшення дисфункції тимуса в умовах неопластичного процесу.

Ключові слова: оксидативний стрес, наночастинки Au/Ag/Fe, тимус, N, N-диметилгідразину дигідрохлорид, індукований канцерогенез товстої кишки.

The work is a fragment of the research project "Morphological and metabolic aspects of carcinogenesis", state registration No. 0123U100070.

According to the latest data from the International Agency for Research on Cancer, approximately 1.9 million new cases of colorectal cancer and more than 900,000 deaths caused by this disease are registered worldwide each year [8]. The initiation and progression of carcinogenesis are closely linked to oxidative stress, which leads to DNA damage, mutation accumulation, genomic instability, and changes in cell proliferative activity [9, 14].

Oxidative stress is defined as an imbalance between the formation of free radicals and reactive metabolites (oxidants or reactive oxygen species (ROS)) and their neutralization by the body's defense systems (antioxidants) [13]. Disruption of this balance can damage key biomolecules and cellular structures, negatively affecting the body's overall function. Under the influence of ROS, lipid peroxidation products are formed, including diene and triene conjugates (DC, TC), thiobarbituric acid reactive substances (TBARS), and Schiff bases (SB) [1, 10]. Their neutralization involves enzymatic components of the antioxidant system – superoxide dismutase (SOD), catalase (CAT), glutathione peroxidase (GPx), and glutathione reductase (GR) – as well as non-enzymatic factors, notably reduced glutathione (GSH), which is crucial for mitigating oxidative stress, preserving redox homeostasis, supporting metabolic detoxification, and modulating immune system activity [5, 11].

The thymus is the central organ of the immune system and is extremely sensitive to oxidative stress. Excessive formation of reactive oxygen species can lead to organ atrophy, thymocyte apoptosis, and impaired differentiation and maturation of T lymphocytes. In addition, oxidative stress can alter the stromal

microenvironment, disrupt positive and negative selection mechanisms, and promote premature thymic involution [15].

In recent years, metal nanoparticles (NPs) have attracted considerable attention as promising alternatives to traditional cancer treatment approaches. Due to their unique physicochemical properties, they show great potential for various therapeutic applications in oncology [7].

The anti-inflammatory and probiotic properties of gold NPs [12], the unique antimicrobial activity of silver NPs [6], and the anti-anemic and probiotic effects of iron NPs are well known [3].

Although many studies have examined the action of NPs of individual metals, data on their effectiveness in nanocomposites, as well as their effects on oxidative stress markers and the morphological state of immune system organs, remain limited.

The purpose of the study was to determine the effect of the Au/Ag/Fe nanocomposite on oxidative stress indicators and the histological state of the thymus under conditions of induced carcinogenesis.

Materials and methods. The study was conducted on 31 outbred sexually mature male white rats with a starting body weight of 190–220 g and an age of approximately 3 months. For modeling N, N-dimethylhydrazine-induced (DMH-induced) colorectal cancer, outbred male rats were used due to the high reproducibility of tumor development and the stability of metabolic and hormonal parameters. Animals were kept under standard vivarium conditions (temperature 22±2°C, relative humidity 50–60 %, 12-h light/dark cycle) in plastic cages with wood shavings bedding, with free access to drinking water and a basal diet ad libitum. All procedures involving animals complied with internationally accepted guidelines and were approved by the Bioethical Committee of Ternopil National Medical University (Protocol No. 75, 01.11.2023). The experiment adhered to the requirements of the European Convention for the Protection of Vertebrate Animals Used for Experimental and Other Scientific Purposes.

The animals were assigned to the following groups:

Group I – intact rats (Intact);

Group II – intact rats with 21 days NPs administration (Intact+NPs);

Group III – rats administered N, N-dimethylhydrazine dihydrochloride for 30 weeks (DMH);

Group IV – rats receiving an intragastric Au/Ag/Fe NP composition daily for 21 days following induced adenocarcinoma (DMH+NPs).

DMH-induced colon adenocarcinoma in situ was modeled by administering N, N-dimethylhydrazine hydrochloride (Sigma-Aldrich Chemie, Japan, batch D161802) dissolved in isotonic sodium chloride solution. The chemical carcinogen was injected subcutaneously into the interscapular region once weekly for 30 weeks at a dose of 7.2 mg/kg body weight (calculated per active compound). Intact animals received 0.1 mL of physiological saline (Yuria-Pharm LLC, Cherkasy, Ukraine) with the same administration schedule. After 30 weeks of DMH treatment, colon adenocarcinoma in situ was confirmed histologically in the experimental rats.

The study utilized a composite containing spherical NPs of silver (d=30 nm), gold (d=30 nm), and iron (d=40 nm) at the following concentrations per 1 mL: 1.6 mg Ag, 0.1 mg Fe, and 3.088 μg Au. Silver nanoparticles were synthesized via tannic-acid reduction of silver nitrate ($AgNO_3$) in the presence of potassium carbonate (K_2CO_3). Gold nanoparticles were obtained by reducing tetrachloroauric (III) acid ($HAuCl_4 \cdot 3H_2O$, ≥99.9 % trace metals basis, Sigma-Aldrich) with trisodium citrate dihydrate in the presence of potassium carbonate. Iron nanoparticles were produced through the reduction of iron (III) chloride with sodium borohydride ($NaBH_4$). The Au/Ag/Fe NP composite used in the experiment was prepared by mechanically combining the individual aqueous dispersions of silver, gold, and iron NPs. Both the source metal NPs and the final composition were verified as non-toxic based on cytotoxicity (MTT assay), genotoxicity (comet assay), mutagenicity (Allium test), and in vitro immunotoxicity assessments [4].

The animals were administered the Au/Ag/Fe nanoparticle dispersion intragastrically once daily for 21 days at a dose of 0.842 mg Ag, 0.0526 mg Fe, and 1.625 μg Au per kilogram of body weight. Before administration, the initial NP mixture was diluted with sterile distilled water at a 1:10 ratio.

Oxidative stress was assessed in thymus homogenates by measuring TBARS, DC, TC, SB, and GSH levels, as well as CAT, SOD, GPx, and GR activities, according to standard methods [2].

The organ was collected from the animals and fixed overnight in 10 % neutral buffered formalin (Biognost, Croatia). Tissue processing was performed using a histoprocessor LOGOSone (Milestone, Italy). For histological examination, 5 μm-thick paraffin sections of the thymus were prepared with a manual rotary microtome AMR 400 (Amos Scientific, Australia), stained with Hematoxylin and Eosin (H&E) (Biognost, Croatia), and analyzed under a Nikon Eclipse Ci light microscope (Nikon, Japan). Images were captured using a Sigeta M3CMOS 14000 digital camera.

Morphometric analysis of the thymic cortex was performed using Fiji software (ImageJ 1.53c, National Institutes of Health, USA) in 155 fields of view (1000 μm² each). Thymocytes were manually counted using the Cell Counter plugin.

Statistical analysis of the data was performed using descriptive statistics and one-way analysis of variance (ANOVA), followed by Tukey's post-hoc test in GraphPad Prism 8 (GraphPad Software, San Diego, CA, USA). Data are presented as mean ± standard error of the mean (M±SEM). Differences were considered statistically significant at $p<0.05$.

Results of the study and their discussion. According to biochemical analyses, DMH-induced carcinogenesis was accompanied by a pronounced increase in lipid and protein peroxidation.

In thymus homogenates, the level of DC in the DMH group reached 2.79±0.14 I.U./g, which was significantly higher ($p=0.003$) than in the intact group 2.15±0.10 I.U./g. Administration of NPs to intact animals did not cause statistically significant changes in DC levels ($p=0.598$). In the DMH+NPs group, a significant decrease in DC concentration was observed compared with the DMH group ($p=0.048$), by 1.16-fold, indicating partial suppression of the primary stage of lipid peroxidation (Fig. 1A).

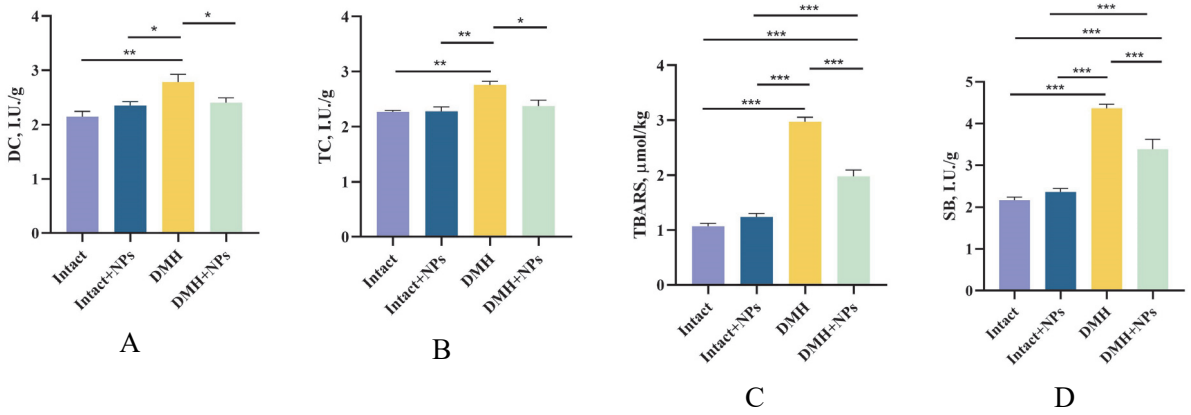

Fig. 1. Levels of lipid peroxidation products in the thymus of rats under experimental conditions. A – diene conjugates (DC), B – triene conjugates (TC), C – thiobarbituric acid reactive substances (TBARS), D – Schiff bases (SB). Data are presented as M±SEM. Differences were considered statistically significant at $p<0.05$ (*), $p<0.01$ (**), and $p<0.001$ (***).

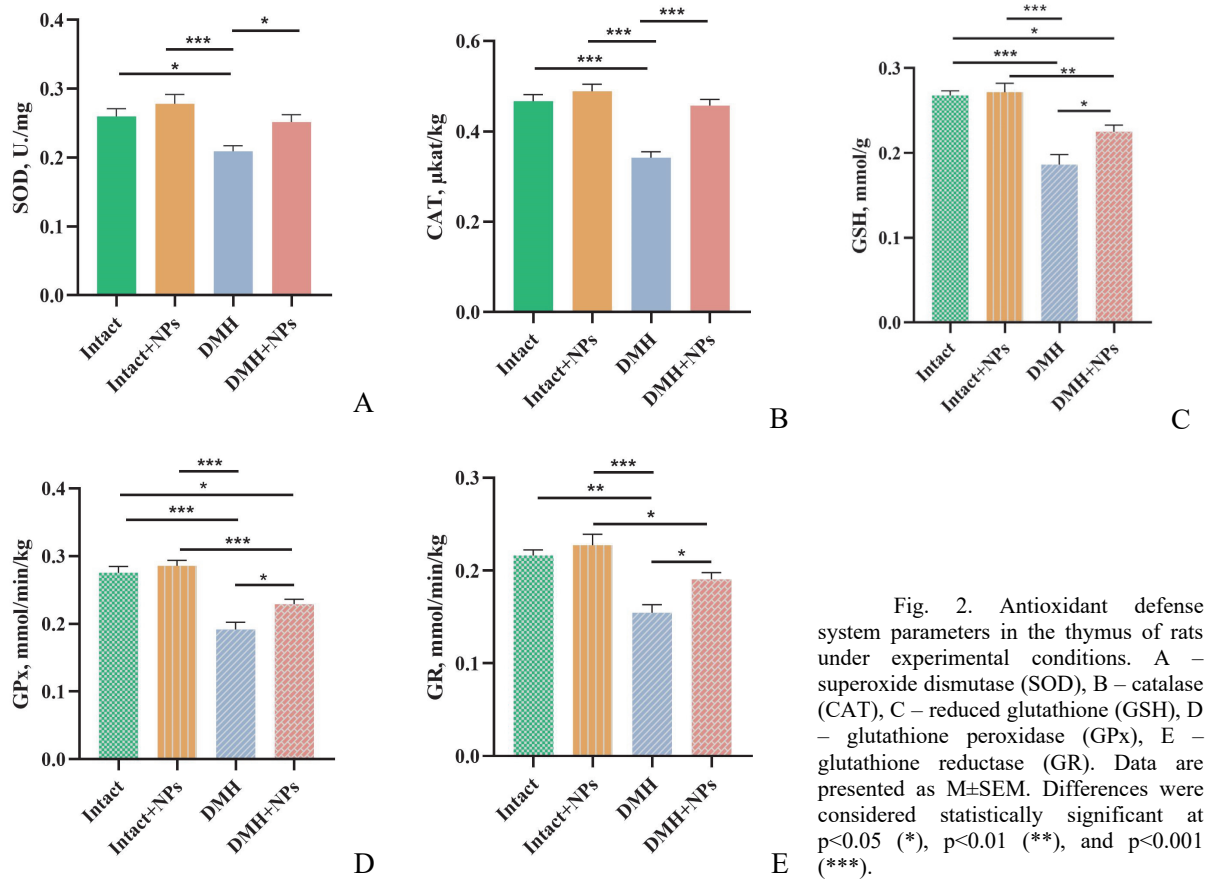

Fig. 2. Antioxidant defense system parameters in the thymus of rats under experimental conditions. A – superoxide dismutase (SOD), B – catalase (CAT), C – reduced glutathione (GSH), D – glutathione peroxidase (GPx), E – glutathione reductase (GR). Data are presented as M±SEM. Differences were considered statistically significant at $p<0.05$ (*), $p<0.01$ (**), and $p<0.001$ (***).

A similar trend was observed for TC. In animals with DMH-induced carcinogenesis, the TC level was 2.76±0.07 I.U./g, which was significantly higher than in the control group ($p=0.007$). Administration of NPs under carcinogenic conditions resulted in a significant reduction of this parameter ($p=0.013$) to 2.38±0.11 I.U./g, although it remained higher than in intact animals (Fig. 1B).

The most pronounced changes were detected for TBARS, markers of the terminal stage of lipid peroxidation. In the DMH group, TBARS levels increased 2.79-fold compared with the intact group ($p<0.0001$). NP administration led to a significant 1.51-fold decrease in TBARS concentration ($p<0.0001$); however, the values remained significantly higher ($p<0.0001$) than control levels (Fig. 1C).

Evaluation of protein oxidative modification showed that the content of SB in the thymus of animals with induced carcinogenesis was maximal 4.37±0.10 I.U./g and exceeded the intact group values by 2.01-fold ($p<0.0001$). Administration of NPs in animals with DMH-induced pathology resulted in a significant 1.29-fold decrease in Schiff base levels ($p<0.001$), indicating attenuation of oxidative damage to protein molecules (Fig. 1D).

Analysis of thymic antioxidant system parameters revealed pronounced disturbances in the prooxidant–antioxidant balance during DMH-induced carcinogenesis.

SOD activity in animals of the DMH group was 0.209±0.008 U./mg. It was significantly reduced compared with the intact group ($p=0.044$), showing a 1.24-fold decrease, which indicates depletion of the first line of enzymatic antioxidant defense (Fig. 2A). Administration of NPs to intact animals was accompanied by a moderate increase in SOD activity to 0.278±0.013 U./mg, which was not statistically significant compared with the control group but was significantly higher than in the DMH group ($p<0.001$). In the DMH+NPs group, SOD activity increased significantly to 0.252±0.011 U./mg compared with the DMH group ($p=0.049$), although it did not reach the level observed in intact animals.

Similar changes were observed for CAT (Fig. 2B). In animals with DMH-induced carcinogenesis, catalase activity was significantly lower than in intact animals ($p<0.0001$), resulting in a 1.37-fold decrease. Administration of NPs in the background of carcinogenesis resulted in a significant increase in enzyme activity ($p<0.0001$) to 0.457±0.013 μkat/kg, indicating partial restoration of the capacity for hydrogen peroxide detoxification.

Evaluation of the non-enzymatic antioxidant defense revealed a marked reduction in GSH content in the thymus of DMH-treated animals compared with the intact group ($p<0.0001$), with a 1.44-fold decrease (Fig. 2C). Administration of NPs to animals with carcinogenesis led to a significant increase in GSH levels ($p=0.034$) by 1.21-fold; however, GSH content remained lower than control values ($p=0.046$).

GPx activity in the DMH group was 0.192±0.011 mmol/min/kg. It was significantly lower than in intact animals ($p<0.0001$), demonstrating a 1.43-fold decrease (Fig. 2D). Treatment with NPs after completion of neoplastic process induction resulted in a significant increase in GPx activity ($p=0.022$) by 1.19-fold, which is consistent with the observed expansion of the GSH pool. A similar trend was observed for GR activity: in the DMH group, it was minimal at 0.155±0.009 mmol/min/kg, whereas in the DMH+NPs group it increased significantly ($p=0.042$) to 0.191±0.007 mmol/min/kg, although it did not reach the level of intact animals (Fig. 2E).

Since oxidative stress is one of the key pathogenetic mechanisms underlying numerous diseases and leads to disruption of the structural organization and functional state of organs, the results of microscopic and morphometric examinations of the thymus in the experimental animal groups are presented below.

Histological analysis demonstrated that intact animals preserved the typical histoarchitecture of the thymus, characterized by a clear distinction between the cortex and medulla of the thymic lobule, a high density of thymocytes in the cortical zone (33.32±0.64 per 10^3 μm²), and numerous cells in the medulla. Administration of NPs to intact animals did not result in significant morphological alterations: histological appearance remained comparable to that of the control group, and thymocyte density did not differ significantly from intact values. At the same time, increased macrophage activity was observed in the connective tissue septa between thymic lobules in this experimental group, which is likely associated with NP administration (Fig. 3A, 3B).

In animals with DMH-induced carcinogenesis, pronounced destructive changes in thymic histology were observed, including a significant ($p<0.0001$) 1.62-fold decrease in thymocyte density compared with intact animals, widening of intercellular spaces, apoptotic and necrotic features, fibrotic changes, and disruption of organ architecture. Administration of NPs to animals with an induced neoplastic process resulted in partial preservation of thymic structure, with more distinct delineation of cortex and medulla, less pronounced destructive changes, and the presence of macrophages within the organ's

connective tissue. Thymocyte density in the cortex of thymic lobules in the DMH+NPs group was 1.16-fold higher ($p<0.001$) than in the DMH group; however, it remained significantly lower ($p<0.0001$), by 1.40-fold, compared with intact animals (Fig. 3A, 3B).

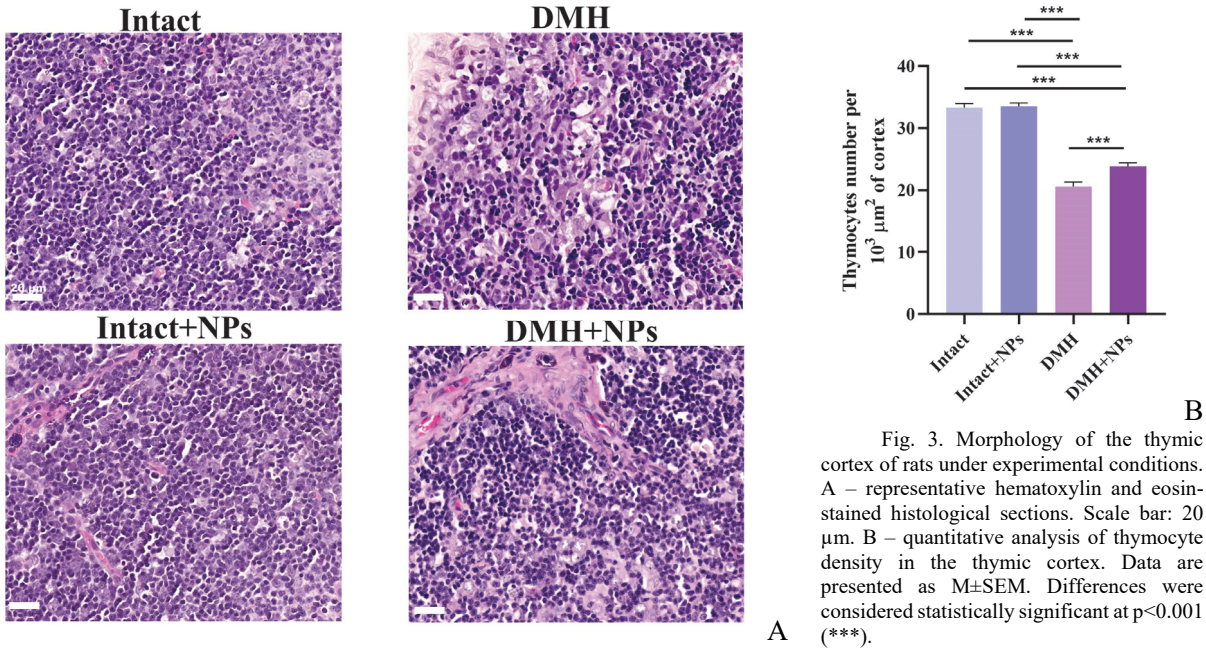

A B

Fig. 3. Morphology of the thymic cortex of rats under experimental conditions. A – representative hematoxylin and eosin-stained histological sections. Scale bar: 20 µm. B – quantitative analysis of thymocyte density in the thymic cortex. Data are presented as M±SEM. Differences were considered statistically significant at $p<0.001$ (***).

The progression of oxidative damage is accompanied by suppression of both the enzymatic and non-enzymatic components of the thymic antioxidant system. Reduced activities of SOD and CAT indicate exhaustion of ROS-inactivating mechanisms. In contrast, a decrease in GSH content, together with diminished GPx and GR activities, reflects impairment of the glutathione system, a key component of cellular redox homeostasis [11]. Given the high sensitivity of thymocytes to oxidative stress, these alterations may underlie disturbances in proliferation, differentiation, and survival of immune system cells [15].

Administration of Au/Ag/Fe nanocomposite to animals with DMH-induced carcinogenesis resulted in a significant reduction in oxidative damage markers and partial restoration of antioxidant defense parameters. The corrective effect of the nanocomposite is likely mediated by attenuation of ROS generation and modulation of redox-sensitive signaling pathways [1, 6, 7]. However, incomplete recovery of these parameters to the levels observed in intact animals indicates persistence of a prooxidant burden under carcinogenic conditions.

Morphological alterations of the thymus, including reduced thymocyte density and disruption of organ architectonics, are consistent with the biochemical findings and reflect functional impairment of this central organ of immunogenesis. Partial restoration of thymic histology and increased thymocyte numbers following NP administration may indicate a protective effect, attributable to their antioxidant and immunomodulatory properties [1, 3, 6]. The absence of adverse effects of NPs on the thymus of intact animals confirms their relative safety at the administered dose [1, 4].

Conclusions

1. DMH-induced carcinogenesis induces pronounced oxidative stress in the thymus, as evidenced by the activation of lipid and protein peroxidation processes: the levels of DC, TC, and TBARS increased by 1.30 ($p=0.003$), 1.22 ($p=0.007$), and 2.79-fold ($p<0.0001$), respectively, compared to intact animals, while the content of SB increased 2.01-fold ($p<0.0001$).

2. Oxidative damage is accompanied by suppression of the thymic antioxidant system. In animals with DMH-induced carcinogenesis, SOD and CAT activities decreased 1.24 ($p=0.044$) and 1.37-fold ($p<0.0001$), respectively, compared to intact values; GSH content and GPx and GR activities decreased by 1.44 ($p<0.0001$), 1.43 ($p<0.0001$), and 1.40-fold ($p=0.002$), indicating disruption of cellular redox homeostasis.

3. Administration of the Au/Ag/Fe nanocomposite during DMH-induced carcinogenesis reduces oxidative stress and partially restores antioxidant defense. In the DMH+NPs group compared to DMH alone, DC, TC, TBARS, and SB levels decreased 1.16 ($p=0.048$), 1.16 ($p=0.007$), 1.50 ($p<0.0001$), and 1.29-fold ($p<0.001$), respectively. At the same time, antioxidant enzyme activities and GSH content increased significantly, though not to control levels.

4. Biochemical alterations correlate with morphological changes in the thymus. DMH-induced carcinogenesis was associated with a 1.62-fold reduction in thymocyte density ($p<0.0001$) and disruption of thymic histoarchitecture. In contrast, NP administration increased thymocyte density by 1.16-fold compared to the DMH group ($p<0.001$), indicating partial immunoprotective effects.

5. These findings suggest potential antioxidant and immunoprotective properties of the Au/Ag/Fe nanocomposite, providing a basis for further experimental studies aimed at correcting oxidative stress and thymic dysfunction under neoplastic conditions.

References

1. Andriichuk IYa, Hrytsyshyn LYe, Ivanchuk IM, Soroka YuV, Lisnychuk NYe. Korehuiucha diia nanochastynok Au/Ag/Fe za umov oksydatyvnoho stresu pry indukovanii adenokartsynomi tovstoi kyshky. Aktualni problemy suchasnoi medytsyny. 2023; 11 :56–64. [in Ukrainian].
2. Vlizlo VV, Fedoruk RS, Ratych IB. Laboratorni metody doslidzhen u biolohii, tvarynnytstvi ta veterynarnii medytsyni: dovidnyk. Lviv: SPOLOM; 2012. 764 p. [in Ukrainian].
3. Doroshenko AM, Dybkova SM, Rieznichenko LS, Gruzina TG, Ulberg ZR, Chekman IS. Vplyv nanochastynok zaliza na stan mikroflory kyshechnyka shchuriv iz zalizodefitsytnoiu anemiieiu. J. Clin. Exp. Med. Res. 2014; 2(3) :292–99. [in Ukrainian].
4. Ryzhenko GF, Dybkova SM, Horbatyuk OI, Andriyashchuk VO, Zhovnir OM, Ukhovska TM, et al. Skryninh nanochastynok metaliv dlia biotekhnolohii veterynarnykh imunobiolohichnykh zasobiv. Bulletin Vet Biotechnol. 2017; 30 :206-13. [in Ukrainian].
5. An X, Yu W, Liu J, Tang D, Yang L, Chen X. Oxidative cell death in cancer: mechanisms and therapeutic opportunities. Cell Death Dis. 2024; 15(8) :556. doi: 10.1038/s41419-024-06939-5.
6. Docea AO, Calina D, Buga AM, Zlatian O, Paoliello MMB, Mogosanu GD, et al. The Effect of Silver Nanoparticles on Antioxidant/Pro-Oxidant Balance in a Murine Model. International journal of molecular sciences. 2020; 21(4) :1233. https://doi.org/10.3390/ijms21041233.
7. Hheidari A, Mohammadi J, Ghodousi M, Mahmoodi M, Ebrahimi S, Pishbin E, Rahdar A. Metal-based nanoparticle in cancer treatment: lessons learned and challenges. Front Bioeng Biotechnol. 2024;12:1436297. doi: 10.3389/fbioe.2024.1436297.
8. International Agency for Research on Cancer. World Health Organisation [Internet]. IARC marks Colorectal Cancer Awareness Month 2025 [updated 2025 February 28; cited 2025 Nov 5]. Available from: https://www.iarc.who.int/news-events/iarc-marks-colorectal-cancer-awareness-month-2025.
9. Iqbal MJ, Kabeer A, Abbas Z, Siddiqui HA, Calina D, Sharifi-Rad J, et al. Interplay of oxidative stress, cellular communication and signaling pathways in cancer. Cell Commun Signal. 2024; 22(1) :7. doi: 10.1186/s12964-023-01398-5.
10. Juan CA, Pérez de la Lastra JM, Plou FJ, Pérez-Lebeña E. The chemistry of reactive oxygen species (ROS) revisited: outlining their role in biological macromolecules (DNA, lipids and proteins) and induced pathologies. Int J Mol Sci. 2021; 22(9) :4642. doi: 10.3390/ijms22094642.
11. Kachur O, Fira L, Lykhatskyi P, Bekus I, Kyryliv M. AUT-M enterosorbent stabilizes glutathione system in vincristine-treated rats with dimethylhydrazine-induced colon cancer. Ukr Biochem J. 2023; 95 :64-72. doi: 10.15407/ubj95.06.064.
12. Milan J, Niemczyk K, Kus-Liśkiewicz M. Treasure on the Earth-Gold Nanoparticles and Their Biomedical Applications. Materials (Basel, Switzerland). 2022; 15(9) :3355. https://doi.org/10.3390/ma15093355.
13. Muscolo A, Mariateresa O, Giulio T, Mariateresa R. Oxidative stress: the role of antioxidant phytochemicals in the prevention and treatment of diseases. Int J Mol Sci. 2024; 25(6) :3264. doi: 10.3390/ijms25063264.
14. Poetsch AR. The genomics of oxidative DNA damage, repair, and resulting mutagenesis. Comput Struct Biotechnol J. 2020; 18 :207–19. doi: 10.1016/j.csbj.2019.12.013.
15. Valdés-Fuentes M, Rodríguez-Martínez E, Rivas-Arancibia S. Redox-Immune Axis and Ozone Pollution: From Oxidative Stress to Thymic Involution and Neurodegeneration. Med Sci (Basel). 2025; 13(4) :293. doi: 10.3390/medsci13040293.

Стаття надійшла 17.11.2024 р.